International Immunopharmacology 129 (2024) 111631

Contents lists available at ScienceDirect

International Immunopharmacology

journal homepage: www.elsevier.com/locate/intimp

Cytotoxicity of fourth-generation anti-Trop2 CAR-T cells against breast cancer

Chalermchai Somboonpatarakun [a,b], Nattaporn Phanthaphol [c], Kwanpirom Suwanchiwasiri [a,d], Boonyanuch Ramwarungkura [a,e], Pornpimon Yuti [a,b], Naravat Poungvarin [f], Peti Thuwajit [g], Mutita Junking [a,b,*], Pa-thai Yenchitsomanus [a,b,*]

[a] Siriraj Center of Research Excellence for Cancer Immunotherapy (SiCORE–CIT), Faculty of Medicine Siriraj Hospital, Mahidol University, Bangkok 10700, Thailand
[b] Division of Molecular Medicine, Research Department, Faculty of Medicine Siriraj Hospital, Mahidol University, Bangkok 10700, Thailand
[c] Institute of Cardiovascular and Medical Science, College of Medical, Veterinary and Life Sciences, University of Glasgow, Glasgow G12 8QQ, Scotland, UK
[d] Graduate Program in Molecular Medicine, Multidisciplinary Unit, Faculty of Science, Mahidol University, Bangkok 10700, Thailand
[e] Graduate Program in Biomedical Sciences, Faculty of Medicine Siriraj Hospital, Mahidol University, Bangkok 10700, Thailand
[f] Department of Clinical Pathology, Faculty of Medicine Siriraj Hospital, Mahidol University, Bangkok 10700, Thailand
[g] Department of Immunology, Faculty of Medicine Siriraj Hospital, Mahidol University, Bangkok 10700, Thailand

ARTICLE INFO

Keywords:
Adoptive T cell therapy
Breast cancer
Cellular immunotherapy
Chimeric antigen receptor (CAR)
Trophoblast cell surface antigen 2 (Trop2)

ABSTRACT

The treatment of breast cancer (BC) remains a formidable challenge due to the emergence of drug resistance, necessitating the exploration of innovative strategies. Chimeric antigen receptor (CAR)-T cell therapy, a groundbreaking approach in hematologic malignancies, is actively under investigation for its potential application in solid tumors, including BC. Trophoblast cell surface antigen 2 (Trop2) has emerged as a promising immunotherapeutic target in various cancers and is notably overexpressed in BC. To enhance therapeutic efficacy in BC, a fourth-generation CAR (CAR4) construct was developed. This CAR4 design incorporates an anti-Trop2 single-chain variable fragment (scFv) fused with three costimulatory domains –CD28/4-1BB/CD27, and CD3ζ. Comparative analysis with the conventional second-generation CAR (CAR2; 28ζ) revealed that anti-Trop2 CAR4 T cells exhibited heightened cytotoxicity and interferon-gamma (IFN-γ) production against Trop2-expressing MCF-7 cells. Notably, anti-Trop2 CAR4-T cells demonstrated superior long-term cytotoxic functionality and proliferative capacity. Crucially, anti-Trop2 CAR4-T cells displayed specific cytotoxicity against Trop2-positive BC cells (MDA-MB-231, HCC70, and MCF-7) in both two-dimensional (2D) and three-dimensional (3D) culture systems. Following antigen-specific killing, these cells markedly secreted interleukin-2 (IL-2), tumor necrosis factor-alpha (TNF-α), IFN-γ, and Granzyme B compared to non-transduced T cells. This study highlights the therapeutic potential of anti-Trop2 CAR4-T cells in adoptive T cell therapy for BC, offering significant promise for the advancement of BC treatment strategies.

1. Introduction

Breast cancer (BC) ranked as the most prevalent malignancy worldwide in 2020, occupying the highest position concerning both its incidence rate and its impact on female mortality [1]. Treatment strategies for BC hinge on the extent of metastasis. Nonmetastatic BC commonly undergoes localized interventions such as surgical resection or radiation therapy to excise tumors. Conversely, managing metastatic BC necessitates a fusion of localized and systemic modalities encompassing chemotherapy, hormone therapy, and immunotherapy [2]. Although existing standard therapies exhibit an approximate curability rate of 70–80 % for early-stage BC patients, those in advanced stages encounter near intractability [3]. The primary drivers of mortality in advanced BC patients are the occurrences of metastasis and recurrence, further exacerbated by the emergence of treatment resistance impeding therapeutic efficacy [4]. Consequently, there is a compelling need to devise innovative strategies that can efficiently mitigate disease relapse, extend survival, and address the challenges faced by individuals with BC.

The significant advancements made in cancer immunotherapy have opened up novel prospects in the domain of BC treatment. Cellular

* Corresponding authors.
E-mail addresses: mutita.jun@mahidol.ac.th (M. Junking), pathai.yen@mahidol.edu (P.-t. Yenchitsomanus).

https://doi.org/10.1016/j.intimp.2024.111631
Received 20 September 2023; Received in revised form 24 January 2024; Accepted 30 January 2024
Available online 14 February 2024

immunotherapy, a pioneering progress within cancer treatment, employs a patient's own immune cells to precisely target cancer cells, represents a paradigm-shifting progression in cancer therapy [5]. Adoptive cell therapy, particularly through the application of autologous T cells engineered with chimeric antigen receptors (CARs), stands as a potent therapeutic approach capable of recognizing cancer cells and effectively exerting cytotoxicity [6]. Notably, the US FDA has approved four CAR-T cell therapies targeting CD19, demonstrating promising clinical outcomes in treating B-cell lymphoid malignancies [7–10]. This triumph in hematological malignancies has attracted the interest of researchers towards extending CAR-T cell immunotherapy to solid tumors [11]. The evolution of CAR-T cells encompasses three generations, each incorporating distinct antigen recognition, spacer, transmembrane, and intracellular domains. The intracellular domain of these CAR generations incorporates differing quantities of co-stimulatory molecules linked to CD3ζ. Remarkably, the second and third generations have exhibited superior anti-tumor effects in comparison to the first generation [12,13]. Prior investigations have also delved into the fourth generation of CAR-T cells, referred to as "T cells redirected for antigen-unrestricted cytokine-initiated killing (TRUCKS)" or "Armored CAR-T cells". These engineered T cells concurrently express the CAR molecule alongside ligands or cytokines to bolster T cell functionality [14]. In this context, we propose an innovative fourth-generation CAR-T cell design that integrates three distinct costimulatory molecules (CD28, 4-1BB, and CD27) linked to CD3ζ. It is noteworthy that our research collective has recently presented findings on the application of fourth-generation CAR-T cells within models of solid tumors [15–18].

The meticulous selection of appropriate antigens presented on cancer cells constitutes a pivotal factor in devising a potent CAR-T cell strategy. This selection processes not only guarantees therapeutic efficacy but also serves to mitigate potential adverse effects. In the context of BC, a range of promising antigens has been identified, encompassing HER2, CD133, mesothelin, MUC1, and cMET. The development of CAR-T cells that specifically target these antigens has been undertaken and is presently navigating clinical trials. However, only a limited amount of publicly available data from these ongoing trials exists in the current landscape [19]. Trophoblast cell-surface antigen 2 (Trop2) is a membrane-associated glycoprotein significantly overexpressed in various epithelial malignancies, including pancreatic cancer [20], colon cancer [21], ovarian carcinoma [22], gastric cancer [23], and breast cancer [24,25]. In contrast, normal epithelial tissues typically exhibit minimal or subdued levels of Trop2 expression [26]. Extensive investigation has elucidated Trop2′s pivotal role in tumor proliferation, invasion, and the metastatic cascade [27]. Moreover, heightened Trop2 expression has been associated with an unfavorable prognosis in BC patients [28]. Notably, the FDA recently approved the anti-Trop2 antibody-drug conjugate, IMMU-132 (sacituzumab govitecan), for the treatment of metastatic triple-negative breast cancer (TNBC) cases that have relapsed or shown resistance to treatment [29]. This underscores the potential of targeting Trop2 with CAR-T cells to enhance BC treatment. Previous reports have detailed the use of anti-Trop2 CAR-T cells in BC and other solid tumors [30], employing a second-generation CAR structure. Despise their capacity to suppress BC cells, the long-term effector function of these CAR-T cells has not been explored to date. Therefore, there is a need for an alternative CAR design that enhances antitumor activity and persistence to improve CAR-T cell function.

This study aimed to investigate Trop2 expression patterns in BC cell lines and evaluate its viability as a potential therapeutic target. To achieve this, we developed Trop2-specific CAR (anti-Trop2 CAR4)-T cells utilizing a fourth-generation configuration. Notably, previous research consistently indicates that fourth-generation CAR constructs exhibit heightened antitumor efficacy and enhanced proliferation compared to their second- and third-generation counterparts [15–18,31]. Our finding revealed that anti-Trop2 CAR4-T cells demonstrated significant cytotoxicity, robust proliferation, and cytokine secretion when confronted with Trop2-expressing BC cells. These results provide compelling empirical evidence supporting the potential therapeutic use of anti-Trop2 CAR4-T cells as an effective and promising approach for treating Trop2-positive cases of BC.

2. Materials and methods

2.1. Cell lines and culture conditions

Breast cancer cell lines (MDA-MB-231, HCC70, and MCF-7) along with human cervical cancer cell (HeLa) were sourced from the American Type Culture Collection (ATCC) located in Manassas, VA, USA. The Lenti-X™ human embryonic kidney (HEK) 293 T cell line, a derivative of HEK293T cells recognized for their heightened transfection efficiency and capacity for producing high-titer viruses, was procured from Takara Bio in Shiga, Japan. These cell lines were cultured with DMEM medium (Gibco; Invitrogen, Carlsbad, CA, USA), except for the HCC70 cell line which was cultured in RPMI-1640 medium (Gibco). Both culture media were supplemented with 10 % heat-inactivated FBS (Gibco), along with 100 U/ml of penicillin and 100 μg/ml of streptomycin (Sigma-Aldrich, St. Louis, MO, USA). Incubation of all cell lines took place at 37 ℃ within a humidified environment enriched with 5 % CO_2.

2.2. Immunofluorescence staining

Trop2 staining was conducted on HeLa cells and three distinct BC cell lines. Briefly, a total of 1.5×10^5 cells were seeded onto sterile coverslips positioned within a 24-well culture plate. These cells were subjected to staining utilizing an anti-Trop2 antibody (rabbit monoclonal, E8Y8S; Cell Signaling, Danvers, MA, USA) at a dilution of 1:500, with 1 % BSA as the diluent. This mixture was allowed to incubate overnight. Subsequently, a washing step was carried out, followed by the application of donkey anti-rabbit IgG-AlexaFlour® 488 (A21206; Thermo Fisher Scientific, Waltham, MA, USA) and Hoechst 33342 (Thermo Fisher Scientific) at an optimal dilution of 1:1000, with an incubation period of 1 h at room temperature (RT). The resulting immunofluorescence images were captured using a Ti-S Intensilight Ri1 NIS-D inverted fluorescent microscope (Nikon, Tokyo, Japan) set at 40 × magnification.

2.3. Generation and expression of lentiviral constructs targeting Trop2

The single-chain antibody variable fragment (scFv) targeting Trop2 (anti-Trop2 scFv) was extracted from the hRS7 antibody sequence [32], renowned for its affinity towards the extramembrane domain of Trop2. To generate the anti-Trop2 scFv, a gene comprising a signal peptide and the scFv was synthesized. This DNA fragment was subsequently integrated into the lentiviral CAR vectors encoding the human CD8 hinge, a CD28 transmembrane domain, and CD28/CD3ζ (CAR2) or CD28/4-1BB/CD27/CD3ζ (CAR4) signaling domains obtained from our previously study [16]. Following construction, the lentiviral vector was introduced into Stbl3 *Escherichia coli* for propagation, screened by colony polymerase chain reaction (PCR), and the accuracy of the sequence was verified through DNA sequencing. Subsequently, these plasmids were transiently transfected into Lenti-X™ HEK293T cells using Lipofectamine3000® (Life Technologies, Carlsbad, CA, USA). The expression of anti-Trop2 CAR proteins was assessed using flow cytometry.

2.4. Lentivirus production

For the production of lentiviruses, the anti-Trop2 CAR2 or the anti-Trop2 CAR4 transfer plasmid was co-transfected into Lenti-X™ HEK293T cells alongside two lentiviral packaging plasmids, namely pMD2.G (12259; Addgene, Watertown, MA, USA) and psPAX2 (12260; Addgene) through a calcium phosphate precipitation method. Following transfection, the supernatants containing the lentiviral particles were collected at 48- and 72-h post-transfection and subsequently filtered using a 0.45 μm PES membrane filter (Jet Biofil, Guangzhou, China). To

concentrate the lentiviral particles, centrifugation was performed at 20000 × g for a duration of 2 h. The quantification of virus titer was accomplished utilizing a qPCR lentiviral titration kit (Applied Biological Materials, Richmond, Canada) in accordance with the guidelines provided by the manufacturer.

2.5. Generation of chimeric antigen receptor T cells

In accordance with the Ethics Committee of Siriraj Institutional Review Board (SIRB) at the Faculty of Medicine Siriraj Hospital, Mahidol University (Certificate of Approval no. Si 253/2022), venous blood samples were ethically obtained from consenting healthy volunteers. Peripheral blood mononuclear cells (PBMCs) were isolated through gradient centrifugation utilizing Lymphoprep™ (Corning, NY, USA) and then cultured in AIM-V medium (Gibco), supplemented with 5 % human AB serum (Sigma-Aldrich, St. Louis, MO, USA). Following separation, non-adherent lymphocytes were activated for a 3-day period using 5 μg/ml of phytohemagglutinin (PHA)-L (Roche, Penzberg, Germany). The activated T cells underwent transduction using lentiviral particles carrying anti-Trop2 CAR4, facilitated by the inclusion of protamine sulfate (Sigma-Aldrich) at a final concentration of 10 μg/ml. These transduced lymphocytes were maintained in AIM-V medium containing IL-2 (20 ng/ml), IL-7 (10 ng/ml), and IL-15 (40 ng/ml). The phenotype and transduction efficiency of the engineered T cells were assessed within 3–5 days post-transduction. For comparative purposes, activated lymphocytes combined with protamine sulfate, but not subjected to lentiviral transduction, were designated as non-transduced (NT) control cells.

2.6. Flow cytometry

Surface expression of Trop2 on BC cell lines was determined using an anti-Trop2 antibody (rabbit monoclonal, E8Y8S; Cell Signaling, Danvers, MA, USA). Subsequent staining was carried out with an Alexa Fluor® 488-conjugated donkey anti-rabbit IgG antibody (A21206; Thermo Fisher Scientific). For the assessment of both anti-Trop2 CAR2 and anti-Trop2 CAR4 proteins expression on transfected Lenti-X™ HEK293T cells and transduced T cells, a goat anti-mouse IgG $F(ab')_2$ antibody conjugated with Alexa Fluor® 647 (115–605-006; Jackson ImmunoResearch, West Grove, PA, USA) was employed. The immunophenotypes of CAR-T cells were characterized through incubation with antibodies directly conjugated to specific markers, including CD3 (UCHT-1; Immunotools, Friesoythe, Germany), CD4 (MEM-241; Immunotools), CD8 (UCHT-4; Immunotools), CD56 (5.1H11; BioLegend, San Diego, CA, USA), CD45RA (HI100; Invitrogen), and CD62L (HI62L; Immunotools). Flow cytometry analysis was conducted using a BD Accuri™ C6 Plus Flow Cytometer (BD Biosciences, San Jose, CA, USA), and the resulting data were processed using FlowJo software (FlowJo LLC, Ashland, OR, USA).

2.7. Short-term cytotoxicity assay

In the short-term cytotoxic experiment, the killing efficiency of anti-Trop2 CAR2-T cells and anti-Trop2 CAR4-T cells against Trop2-expressing BC cells was evaluated using crystal violet staining. Initially, target tumor cells (1×10^4) were seeded into individual wells of a 96-well plate and co-cultured with CAR-T cells for 24 h at various effector-to-target (E:T) ratios, including 1:4, 1:2, 1.25:1, 2.5:1, and 5:1. Following the co-culture period, the culture medium was aspirated, and the remaining adherent cells were stained with crystal violet for 20 min.

The resultant stained cells were dissolved in methanol, and their optical density (OD) was measured at 595 nm using a Sunrise™ Absorbance Reader (Tecan, Männedorf, Switzerland). Subsequent analysis was performed with Gen5™ software (BioTek Instruments, Winooski, VT, USA). The percentage of cytotoxicity was calculated using the following formula:

$$\%\ Cytotoxicity = \left(1 - \frac{OD[target\ cells\ with\ effector\ cells]}{OD[target\ cells\ alone]}\right) \times 100$$

2.8. Human IFN-γ enzyme-linked immunospot (ELISpot) assay

IFN-γ ELISpot assays were conducted using a human IFN-γ ELISpot^{BASIC} kit (Mabtech, AB, Sweden) following the manufacturer's guidelines. Briefly, PVDF membrane ELISpot plates (Millipore, UK) were coated overnight with 15 μg/ml anti-human IFN-γ (Mabtech, AB, Sweden) at 4 °C. Target cells, HeLa or MCF-7, were added to each CAR T cells at E:T ratio of 5:1 and cultured at 37 °C for 24 h. The secreted IFN-γ was detected by adding 1 μg/ml biotinylated mAb 7-B6-1-biotin and incubated for 2 h, followed by 1 μg/ml streptavidin alkaline phosphatase for 1 h. Spots were visualized after incubation with the substrate BCIP/NBT-plus for 10 min. Color development was halted with a water wash, and the plate was air-dried overnight at RT, avoiding exposure to light. ELISpot plates were scanned using a CTL ELISpot reader (Cellular Technology Limited, USA) within 24–96 h, and spot counts were subsequently analyzed using Immunospot 3.1 software.

2.9. Long-term cytotoxicity assay

To evaluate the sustained cytotoxic potential of anti-Trop2 CAR2-T and anti-Trop2 CAR4-T cells following prolonged incubation with Trop2-positive cells, MCF-7 cells were co-cultured for 6 days at E:T of 1:4. Harvested cells at 2-, 4-, and 6-day intervals were stained with anti-CD3 and anti-PD-1 to assess PD-1 levels on the effector T cells. Absolute numbers of remaining tumor cells were determined by flow cytometry using counting beads (123count™ eBeads Counting Beads; Thermo Fisher Scientific), following the manufacturer's instructions. Additionally, an alternative method for measuring long-term cytotoxicity involved crystal violet staining during the same incubation period.

2.10. T cell proliferation assay

To examine the proliferation of CAR-T cells in response to tumor cells expressing specific antigens, a carboxyfluorescein diacetate succinimidyl ester (CFSE) proliferation assay was conducted. Initially, anti-Trop2 CAR2-T, anti-Trop2 CAR4-T, and non-transduced (NT-T) cells were labeled with CFSE (Invitrogen). These labeled cells were then co-cultured with HeLa or MCF-7 cells at an E:T ratio of 2:1 for 6 days without the addition of extra exogenous cytokines. After 3- and 6-day incubations, the CFSE-labeled T cells were harvested, and T-cell proliferation was assessed by detecting the decreasing CFSE fluorescence intensity using flow cytometry.

2.11. Three-dimension spheroid killing assay

BC cells were subjected to staining with CellTracker™ Green CMFDA Dye (Thermo Fisher Scientific) for a duration of 30 min. Following labeling, the marked cells were combined with 2.5 % Matrigel (Corning) and then introduced into ultra-low attachment 96-well round-bottomed plates (Corning). Over a span of 48 h, the plates were cultured to facilitate the formation of individual spheroids. These cancer spheroids were subsequently co-cultured with anti-Trop2 CAR4-T cells, maintaining an E:T ratio of 5:1, and propidium iodide (PI) was concurrently employed for visualizing cell death. For comparative purposes, cancer spheroids were also treated with 0.1 % Triton-X 100 to establish total tumor cell death. To assess the progression of events, fluorescence images were captured at 24 h and 48 h utilizing a confocal microscope (Nikon, Melville, NY, USA). The mean fluorescence intensity (MFI) of PI was quantitatively analyzed using NIS-Elements software (Nikon). Cytotoxicity evaluation was conducted according to the following formula:

$$\%Specific\ cytolysis = \left(\frac{experimental\ MFI - spontaneous\ MFI}{maximum\ MFI - spontaneous\ MFI}\right) \times 100$$

The experimental MFIs were indicated by the MFIs of cancer spheroids co-cultured with effector cells. In contrast, the spontaneous MFIs referred to the MFIs of cancer spheroids co-cultured without effector cells. The maximum MFI was determined as the MFI of spheroid treated with 0.1 % Triton-X 100.

2.12. Cytokine release assay

To examine cytokine release, effector cells were co-cultured with MCF-7 cells at a 5:1 E:T ratio for 24 h. Subsequently, the co-culture supernatants were harvested, and the concentrations of IL-10, IL-6, IL-2, TNF-α, IFN-γ, and Granzyme B were assessed utilizing the LEGENDplex™ Human CD8/NK Panel (#741065, BioLegend). In brief, the supernatant samples were subjected to incubation with beads characterized by known size and fluorescence properties at RT for 2 h. Following a thorough washing step, biotinylated detection antibodies and streptavidin–phycoerythrin (SA-PE) were sequentially introduced. Subsequently, the fluorescence intensity of the PE signal emitted by each bead population was measured using a CytoFLEX flow cytometer (Beckman Coulter, Atlanta, GA, USA). Cytokine levels were subsequently quantified based on established standard curves.

2.13. Statistical analysis

Student's *t*-test (two groups) or an ANOVA with Tukey's multiple comparison tests (three or more groups) was used to determine statistical significance. All statistical analyses were executed utilizing GraphPad Prism 7.0 software (GraphPad Software, La Jolla, CA, USA). The outcomes are presented as the mean ± standard error of the mean (SEM), derived from a minimum of three distinct experiments. *P* values < 0.05 were considered statistically significant for all tests.

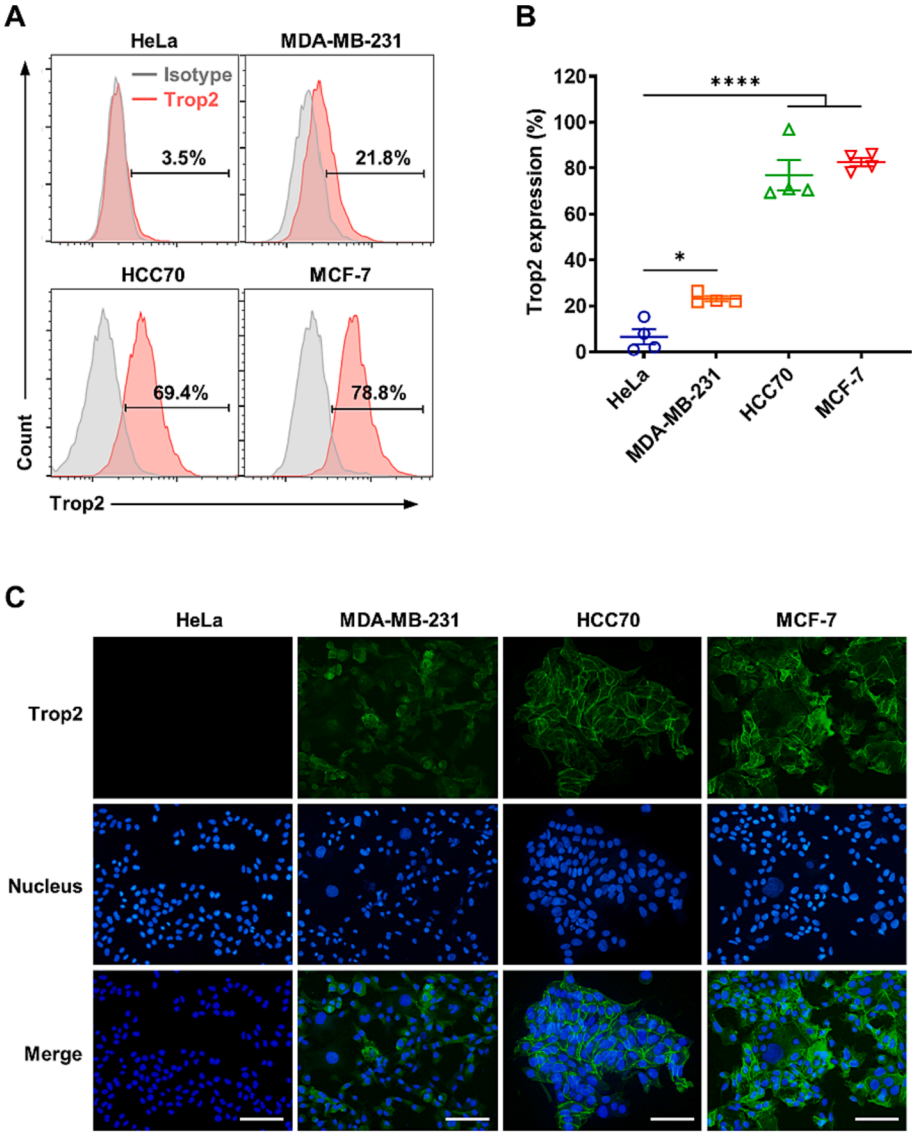

Fig. 1. Assessment of Trop2 protein expression in human BCs (MDA-MB-231, HCC70, and MFC-7) cells and cervical cancer (HeLa) cells using flow cytometry and immunofluorescence staining. (A) Flow cytometry histogram illustrating the surface expression of Trop2 (depicted in red) juxtaposed with the corresponding isotype control (presented in gray). (B) Quantification of Trop2-positive cell proportions was derived from four distinct experimental iterations. The findings are presented as the mean ± standard error of mean (SEM). Statistical significance was determined using the one-way analysis of variance (ANOVA) (*$p < 0.05$, ****$p < 0.0001$). (C) Immunofluorescence micrographs exhibiting membranous Trop2 expression, visualized through anti-Trop2 monoclonal antibody staining (depicted in green), in both BC and HeLa cell lines. Nuclei are counterstained using Hoechst 33342 (depicted in blue). Scale bars correspond to 100 μm.

3. Results

3.1. Expression of Trop2 in breast cancer cell lines

Flow cytometry and immunofluorescence staining were employed to evaluate the presence of the Trop2 protein in BC cell lines, including MDA-MB-231, HCC70, and MFC-7. As a negative control for Trop2 expression, the human cervical cancer cell line, HeLa, was utilized. Our analysis revealed intermediate Trop2 expression in MDA-MB-231 (23.2 ± 1.1 %, $p = 0.0263$) and high expression in HCC70 (77.0 ± 6.7 %, $p < 0.0001$) and MFC-7 (82.7 ± 1.8 %, $p < 0.0001$) compared to HeLa cells (6.6 ± 3.3 %) (Fig. 1A and B). Immunofluorescence staining results supported the surface expression findings obtained via flow cytometry. Specifically, Trop2 was observed on the cellular membrane of MDA-MB-231, HCC70, and MFC-7, while no detectable Trop2 expression was observed in HeLa cell (Fig. 1C).

3.2. Production and characterization of anti-Trop2 CAR4-T cells

Anti-Trop2 CAR2-T and anti-Trop2 CAR4-T cells were generated using lentiviral constructs. The schematic diagram illustrating the anti-Trop2 CAR constructs within the lentiviral vector is presented in Fig. 2A. Successful translation was confirmed in Lenti-X^{TM} HEK293T cells through flow cytometry using an anti-human F(ab′)$_2$ antibody. Results demonstrated significant expression of anti-Trop2 CAR2 and anti-Trop2 CAR4 proteins on the surface of Lenti-X^{TM} HEK293T cells compared to untransfected cells (Supplementary Fig. S1C).

For the production of anti-Trop2 CAR-T cells, primary human lymphocytes from PBMCs of healthy donors were transduced with a lentiviral vector encoding either anti-Trop2 CAR2 or anti-Trop2 CAR4 proteins. Representative flow cytometric plots illustrating this process are shown in Fig. 2B. Data from three independent donors revealed a transduction efficiency of 87.47 ± 5.9 % for anti-Trop2 CAR2 and 84.87 ± 2.1 % for anti-Trop2 CAR4, compared to NT-T cells (both $p < 0.0001$) (Fig. 2B and C).

Subsequently, the immunophenotypic characteristics of anti-Trop2 CAR-T cells were analyzed, focusing on key T cell markers and differentiation indicators, specifically CD45RA and CD62L, to assess the immunocompetence of the final CAR-T cell products. Following T cell expansion, the proportion of cytotoxic T cells ($CD3^+CD56^-CD8^+$) within the NT-T cell group was 80.04 ± 0.9 %, anti-Trop2 CAR2-T cell group was 80.73 ± 2.9 %, and anti-Trop2 CAR4-T cell group was 80.65 ± 1.8 %, significantly higher than observed in freshly isolated PBMCs (25.14 ± 3.9 %, $p < 0.0001$). In contrast, the percentages of helper T cells ($CD3^+CD56^-CD4^+$) in the NT-T cell group, anti-Trop2 CAR2-T cell group, and anti-Trop2 CAR4-T cell group were 20.19 ± 3.3 %, 19.13 ± 2.2 %, and 20.88 ± 3.5 %, respectively, compared to 65.6 ± 5.9 % within PBMCs ($p = 0.0002$) (Fig. 2D).

Furthermore, the population of $CD45RA^-CD62L^+$ central memory T cell (Tcm) significantly increased within anti-Trop2 CAR2-T cells (55.71 ± 1.7 %, $p = 0.0023$) and anti-Trop2 CAR4-T cells (55.79 ± 7.1 %, $p = 0.0022$), compared to levels in PBMCs (19.33 ± 40 %). Conversely, $CD45RA^+CD62L^+$ naïve T cells in anti-Trop2 CAR2-T and anti-Trop2 CAR4-T cells were reduced to 28.52 ± 2.3 % and 27.76 ± 2.0 %, respectively (both $p < 0.0001$), compared to PBMCs at 55.97 ± 1.9 % (Fig. 2E).

3.3. Enhanced antitumor effectiveness demonstrated by anti-Trop2 CAR4-T cells

To assess the comparative efficacy of anti-Trop2 CAR2-T and anti-Trop2 CAR4-T cells in targeting Trop2-expressing BC cells, we conducted co-culture experiments with each CAR-T generation and Trop2-high MCF-7 cells, along with Trop2-negative HeLa cells. Results revealed that both CAR-T generations, derived from three donors, effectively eliminated MCF-7 cells compared to control NT-T cells, while demonstrating minimal cytotoxicity towards HeLa cells (Supplementary Fig. S2). The cytotoxicity of anti-Trop2 CAR4-T cells against MCF-7 cells was significantly higher than that of anti-Trop2 CAR2-T cells at E:T ratios of 1.25:1 ($p = 0.0007$), 2.5:1 ($p < 0.0001$), and 5:1 ($p < 0.0001$) (Fig. 3A).

Furthermore, we assessed IFN-γ production by CAR-T cells in response to Trop2-expressing target cells using an ELISpot assay (Fig. 3B and C). The results indicated a significant increase in IFN-γ production in both anti-Trop2 CAR-T cell populations after co-incubation with MCF-7 cells, compared to NT cells. Conversely, there was no significant difference in spot counts among the three effector T cell populations when exposed to HeLa cells. Notably, anti-Trop2 CAR4-T cells exhibited a significantly higher number of IFN-γ ELISpots (448.3 ± 27.4 spots/2 × 10^4 T cells) compared to anti-Trop2 CAR2-T cells (231.0 ± 27.02 spots/2 × 10^4 T cells) ($p < 0.0001$).

3.4. Anti-Trop2 CAR4-T cells exhibit prolonged antitumor responses and enhanced proliferative capacity compared to anti-Trop2 CAR2-T cells

To assess whether anti-Trop2 CAR4-T cells confer enhanced long-term effector function compared to anti-Trop2 CAR2-T cells, an extended co-culture assay was conducted. NT-T, anti-Trop2 CAR2-T, and anti-Trop2 CAR4-T cells were co-cultured with Trop2-expressing MCF-7 cells for 6 days, during which the exhaustion marker expression on CAR-T cells was determined (Fig. 4). Results demonstrated a time-dependent reduction in MCF-7 cell numbers upon co-culture with both anti-Trop2 CAR-T cell populations. On day 6, both CAR2-T cells (3.03 ± 0.27 × 10^3 cells) and CAR4-T cells (2.47 ± 1.22 × 10^3 cells) significantly reduced MCF-7 populations compared to NT-T controls (231.2 ± 20.58 × 10^3 cells, $p = 0.0004$). Notably, CAR4-T cells exhibited superior MCF-7 elimination at earlier time points, with significantly lower cell numbers compared to CAR2-T cells on day 2 (78.40 ± 9.9 × 10^3 cells vs. 32.43 ± 10.9 × 10^3 cells, $p = 0.0353$) and day 4 (35.57 ± 7.0 × 10^3 cells vs. 5.80 ± 2.5 × 10^3 cells, $p = 0.0164$) (Fig. 4A). Long-term cytotoxicity against Trop2-negative HeLa and Trop2-positive MCF-7 cells using crystal violet staining confirmed higher cytotoxicity of anti-Trop2 CAR4-T cells against MCF-7 cells compared to anti-Trop2 CAR2-T cells at both day 2 and 4 after co-culture (day 2: 36.80 ± 2.6 % vs. 19.87 ± 2.3 %, $p = 0.0389$; day 4: 72.42 ± 5.2 % vs. 54.03 ± 9.5 %, $p = 0.0243$) (Supplementary Fig. S4C and D), supporting the enhanced long-term anti-tumor activity of anti-Trop2 CAR4-T cells. Furthermore, flow cytometry analysis on day 6 revealed significantly lower PD-1 expression in anti-Trop2 CAR4-T cells (34.57 ± 9.9 %) compared to anti-Trop2 CAR2-T cells (53.90 ± 14.5 %, $p = 0.0049$) (Fig. 4B). This reduced exhaustion marker expression likely contributed to their superior long-term tumor-killing activity observed in Fig. 4A, emphasizing the potential of the CAR4 design to enhance sustained anti-tumor efficacy.

To further investigate whether the CAR4 design promotes long-term effector function, a CFSE proliferation assay was performed. Both CAR-T generations demonstrated significantly higher antigen-specific proliferation compared to NT-T cells during co-culture with MCF-7 cells, while remaining in a quiescent state when exposed to HeLa cells (Fig. 5). Notably, anti-Trop2 CAR4-T cells exhibited a significantly higher proliferation rate of 85.73 ± 4.8 % on day 6 compared to CAR2-T cells' rate of 68.57 ± 2.9 % ($p = 0.0034$). Therefore, anti-Trop2 CAR4-T cells were selected for further investigation based on their superior cytotoxicity and proliferative advantage.

3.5. Antitumor efficacy and cytokine production induced by anti-Trop2 CAR4-T cells targeting Trop2-expressing cells

To assess the efficacy of anti-Trop2 CAR4-T cells against both Trop2-expressing BC cell lines (MDA-MB-231, HCC70, and MCF-7) and Trop2-negative HeLa cells, a crystal violet staining assay was conducted. During the co-culture, we exposed the cells either NT-T cells or anti-

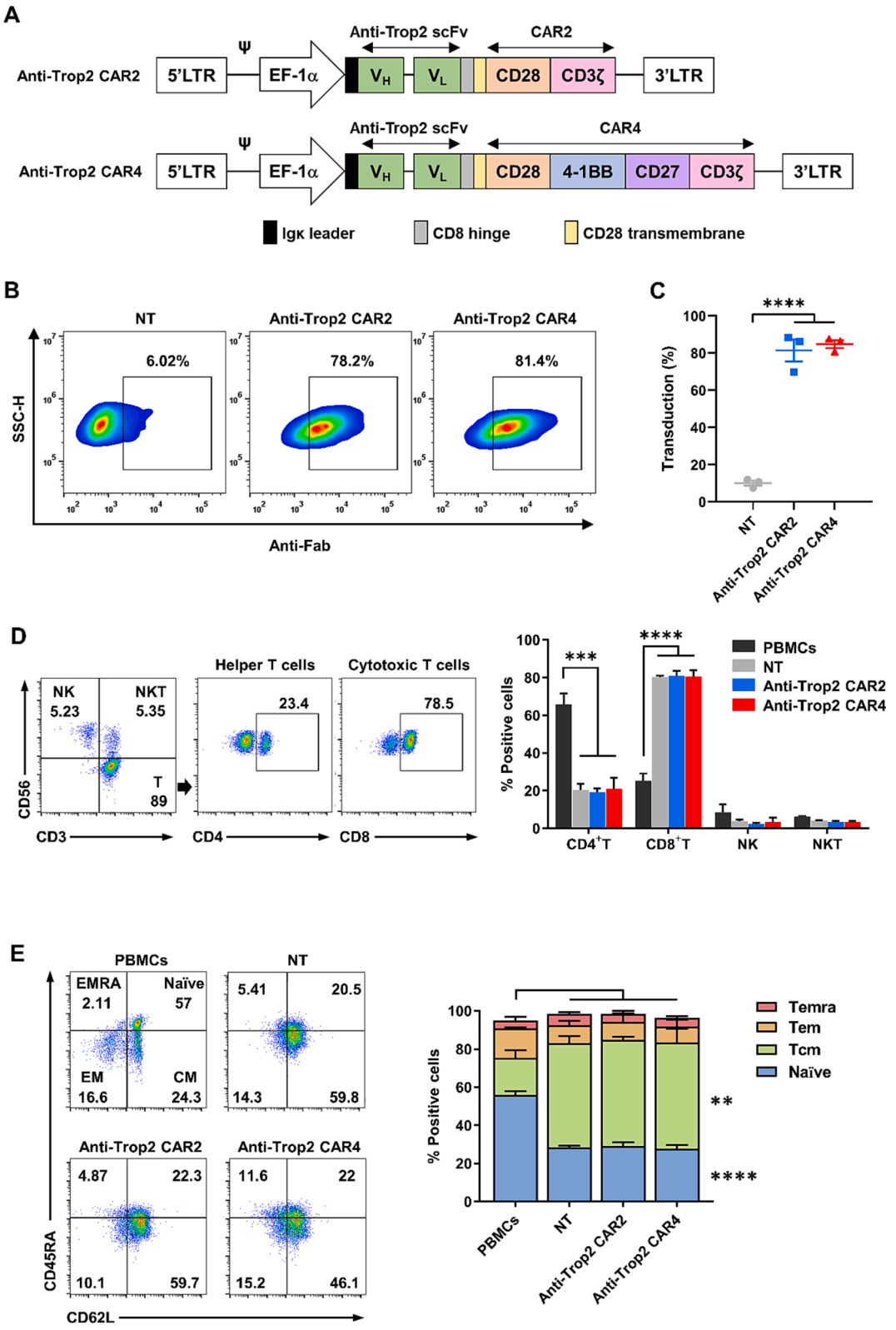

Fig. 2. Generation and characterization of anti-Trop2 CAR-T cells. (A) Schematic representation of the anti-Trop2 CAR2 and anti-Trop2 CAR4 constructs. The sequence encoding the anti-Trop2 single-chain variable fragment (scFv) was incorporated into lentiviral vectors, aligning with the CD28 (CAR2) or CD28, 4-1BB, and CD27 (CAR4) costimulatory domains, in conjunction with the CD3ζ intracellular domain. (B) Flow cytometry-based assessment of representative transduction efficiency of NT-T (gray), anti-Trop2 CAR2-T (blue), and anti-Trop2 CAR4-T (red) cells using the Alexa Fluor® 647-conjugated anti-human F(ab′)$_2$ antibody. (C) Quantification of anti-Trop2 CAR surface expression (n = 3). (D) Cellular subset gating for NK cells, NKT cells, helper T cell, and cytotoxic T cells (left), with corresponding quantification in PBMCs, NT-T cells, anti-Trop2 CAR2-T cells, and anti-Trop2 CAR4-T cells (right). (E) Identification of T cell differentiation stage, including CD45RA$^-$CD62L$^-$ terminal-differentiated T cells (Temra), CD45RA$^+$CD62L$^+$ naïve T cells, CD45RA$^+$CD62L$^-$ effector memory T cells (Tem), and CD45RA$^-$CD62L$^+$ central memory T cells (Tcm). Results are summarized as mean ± SEM from three independent experiments. Statistical differences were evaluated using one-way ANOVA, with asterisks indicating specific p values: $^{**}p < 0.01$, $^{***}p < 0.001$, and $^{****}p < 0.0001$.

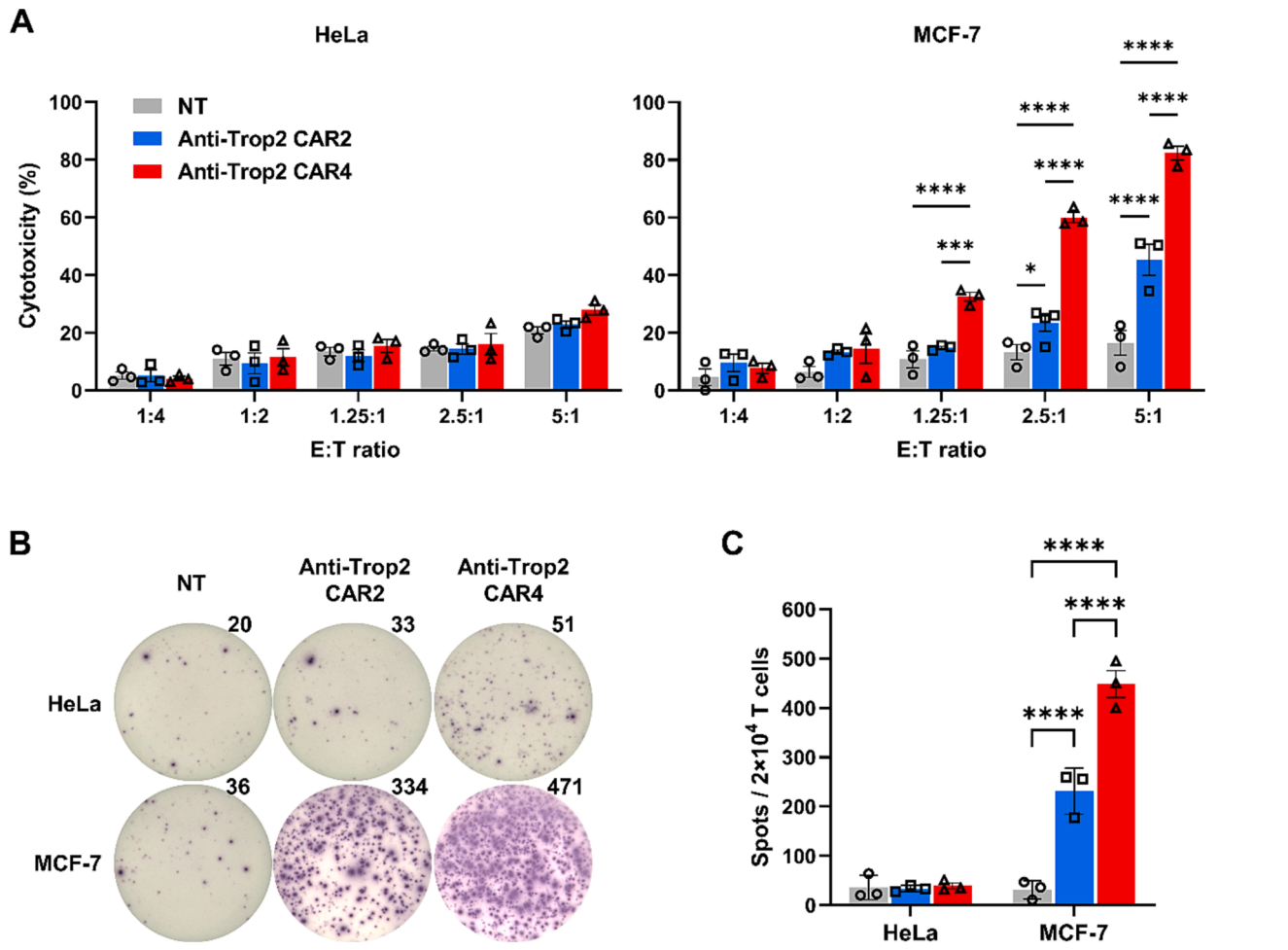

Fig. 3. Cytotoxic effectiveness of anti-Trop2 CAR-T cells against Trop2-expressing BC cell lines. (A) Killing activities of NT-T, anti-Trop2 CAR2-T, and anti-Trop2 CAR4-T cells against HeLa and MCF-7 cells after 24 h of co-culture at various effector-to-target (E:T) ratios (n = 3). The horizontal axis represents the ratio of effector cells to target cells, and the vertical axis represents the percentage of cytotoxicity. (B) Representative images and spot counts from the IFN-γ ELISpot assay. NT-T, anti-Trop2 CAR2-T, and anti-Trop2 CAR4-T cells at concentrations of 2×10^4 cells/well were co-cultured with HeLa (top) or MCF-7 (bottom) cells for 24 h at an E:T = 5:1 and IFN-γ positive spots were counted. Scanned images of the ELISpot plate form all three donors are presented in supplementary Fig. S3. (C) Bar graphs showing the number of IFN-γ positive spots from three independent experiments. All data with error bars denote SEM, and results were compared using two-way ANOVA. $*p < 0.05$, $***p < 0.001$, $****p < 0.0001$.

Trop2 CAR4-T cells at varying E:T ratios (1.25:1, 2.5:1, 5:1) over a 24-h period. Subsequently, we evaluated the viability of the target cells using crystal violet staining. Cytotoxicity levels were determined by dissolving the crystal violet dye from surviving target cells and measuring the optical density (OD) at 595 nm. As expected, anti-Trop2 CAR4-T cells exhibited minimal cytotoxicity against HeLa cells, even with increasing E:T ratios (5.7 ± 2.7 %, 13.2 ± 2.5 %, and 14.5 ± 4.7 %, respectively). Similarly, NT-T cells demonstrated cytotoxicity against HeLa cells at rates of 6.4 ± 1.7, 7.7 ± 4.1 %, and 11.3 ± 2.5 %, respectively (Fig. 6A). In contrast, anti-Trop2 CAR4-T cells exhibited dose-dependent killing of Trop2-positive BC cells with varying Trop2 protein expression levels (Fig. 6B-D). For instance, the cytotoxicity of anti-Trop2 CAR4-T cells against MDA-MB-231 cells increased to 26.4 ± 3.3 % ($P = 0.0011$) at an E:T ratio of 5:1, compared to NT-T cells (10.7 ± 3.9 %) (Fig. 6B). Furthermore, the cytotoxicity of anti-Trop2 CAR4-T cells against HCC70 cells was evident at levels of 32.3 ± 5.0 % ($P = 0.0151$) and 40.8 ± 6.2 % ($P = 0.0001$) at E:T ratios of 2.5:1 and 5:1, respectively, in comparison to NT-T cells (Fig. 6C). Likewise, anti-Trop2 CAR4-T cells exhibited substantial cytotoxicity against MCF-7 cells, reaching 28.2 ± 3.5 % ($P = 0.0012$) and 55.4 ± 1.2 % ($P < 0.0001$) at E:T ratios of 2.5:1 and 5:1, respectively, compared to the cytotoxicity of NT-T cells (Fig. 6D).

To assess the release of cytokines and cytolytic molecules by NT-T and anti-Trop2 CAR4-T cells when exposed to Trop2-expressing cells, we conducted a cytokine bead array analysis (Fig. 6E). Our data clearly indicate that the levels of IL-2, TNF-α, IFN-γ and Granzyme B in the culture supernatants of anti-Trop2 CAR4-T cells co-cultured with MCF-7 cells were significantly elevated (507.6 ± 74.4 pg/ml, 240.2 ± 117.3 pg/ml, 6951 ± 416.3 pg/ml, and 4654 ± 1372 pg/ml, respectively) compared to of NT-T cells, where these values were 11.2 ± 5.8 pg/ml ($P = 0.0027$), 2.2 ± 0.4 pg/ml ($P = 0.0320$), 28.1 ± 10.2 pg/ml ($P < 0.001$), and 662.9 ± 128.2 pg/ml ($P = 0.0443$), respectively.

3.6. *Efficacy of anti-Trop2 CAR4-T cells in eliminating Trop2-expressing breast cancer cells within three-dimensional spheroid culture*

The conventional two-dimensional (2D) culture model, where cells grow in a single layer, may not faithfully replicate *in vivo* conditions which involve intricate cell-extracellular matrix interactions. To address this limitation, we employed three-dimensional (3D) BC spheroids that simulate solid tumor structures for evaluating the efficacy of anti-Trop2 CAR4-T cells against tumors. These 3D spheroids were created by embedding CMFDA-labeled HeLa, MDA-MB-231, HCC70, and MCF-7 cells in Matrigel, followed by a 2-day culture period. Subsequently, these spheroids were co-cultured with anti-Trop2 CAR4-T cells alongside staining with PI. The cellular demise within tumor spheroids, identified by the presence of red-fluorescent PI staining, was monitored

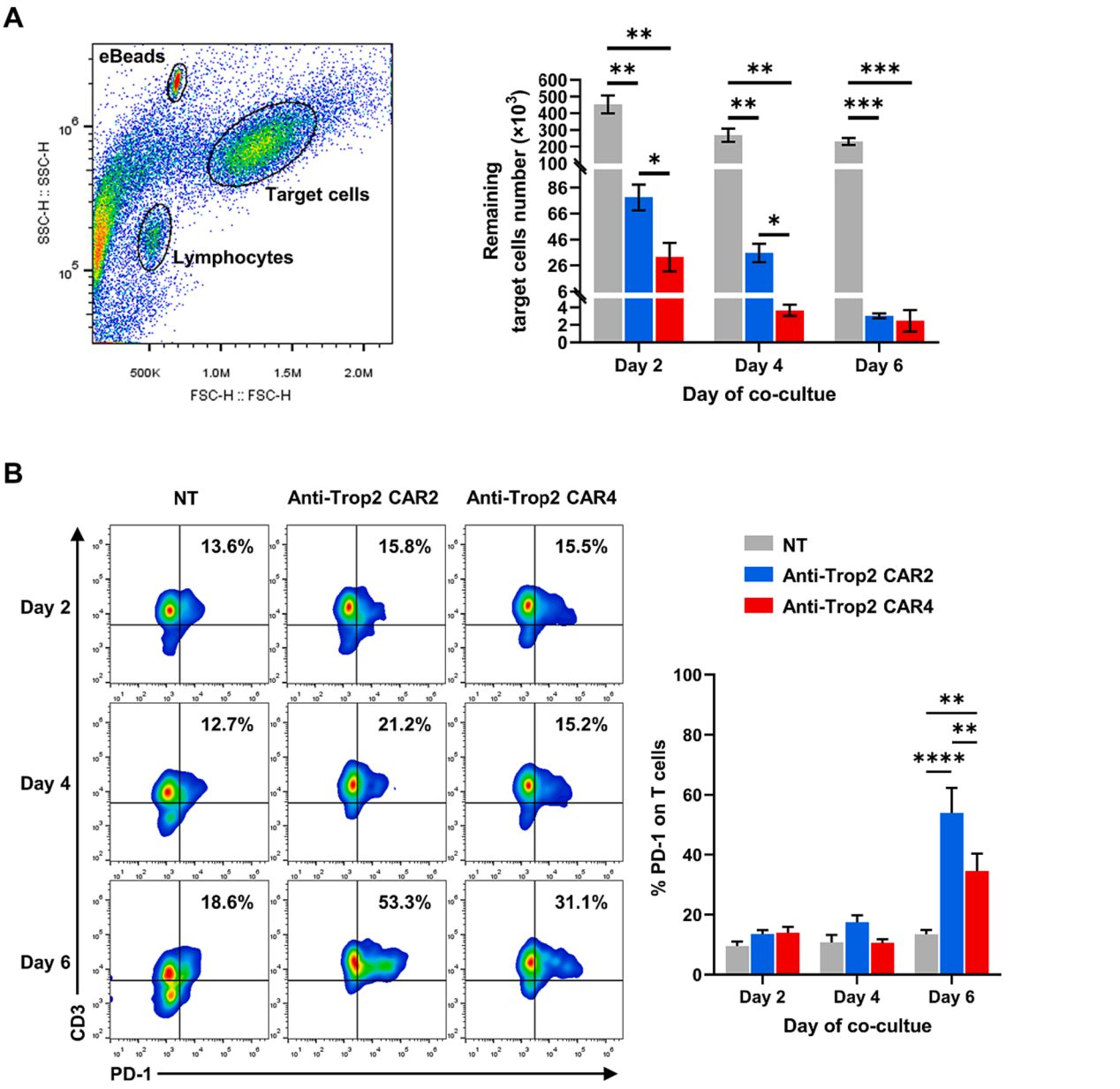

Fig. 4. Enhanced antitumor efficiency of anti-Trop2 CAR4-T cells following prolonged exposure to Trop2-expressing cells. (A) Gating strategy for the quantification of remaining MCF-7 target cells after long-term co-culture with NT-T, anti-Trop2 CAR2-T, and anti-Trop2 CAR4-T cells at an E:T ratio of 1:4. The quantity of remaining target cells was assessed using counting beads every 2 days until day 6, with results compared using unpaired *t*-test. (B) Examination of PD-1 expression on effector T cells. All data with error bars represent the mean ± SEM of three independent experiments. $*p < 0.05$, $**p < 0.01$, $***p < 0.001$, $****p < 0.0001$.

under a confocal microscope at 24 h and 48 h. The findings indicated that the green-fluorescent 3D spheroids consisting of HeLa cells were unaffected by anti-Trop2 CAR4-T cells. Conversely, the 3D spheroids derived from MDA-MB-231, HCC70, and MCF-7 cells exhibited regions with red-fluorescent staining, indicative of their susceptibility to elimination by anti-Trop2 CAR4-T cells (Fig. 7A). Additionally, the intensity of green fluorescence emitted by BC cells markedly diminished, signifying the demise of tumor cells. Calculations of cytotoxicity percentages were derived from mean fluorescence intensities of PI-stained spheroids for each condition. Notably, minimal cytotoxicity was noted when anti-Trop2 CAR4-T cells were co-cultured with Trop2-negative HeLa spheroids for 48 h (Fig. 7B). In contrast, anti-Trop2 CAR4-T cells displayed a time-dependent escalation in cytotoxicity against Trop2-positive MDA-MB-231 spheroids, surpassing the cytotoxic activity of NT-T cells at 48 h (24.3 ± 4.0 % vs. 5.7 ± 3.9 %, $P = 0.0051$; Fig. 7C). This pattern was replicated in HCC70 cell spheroids (47.9 ± 7.6 % vs. 6.8 ± 4.9 %, $P = 0.0005$; Fig. 7D). Notably, anti-Trop2 CAR4-T cells demonstrated marked tumor cell eradication in Trop2-expressing MCF-7 cells after 24 h and 48 h of co-culture (15.3 ± 2.9 % and 43.3 ± 1.7 %, respectively), in comparison to NT-T cells (1.7 ± 1.0 %, $P = 0.0048$ and 5.2 ± 2.6 %, $P < 0.0001$; Fig. 7E).

4. Discussion

Breast cancer has emerged as a significant global health concern, with increasing incidence rates worldwide [33]. While adoptive CAR-T cell therapy has shown promise in treating hematologic malignancies [34], achieving similar effectiveness in solid tumors poses a considerable challenge. Despite extensive exploration in preclinical and clinical trials for BC, CAR-T cell-based immunotherapy has struggled to replicate the success observed with CD19 CAR-T cells in hematopoietic malignancies [19]. Two major obstacles impeding the potency of CAR-T cells

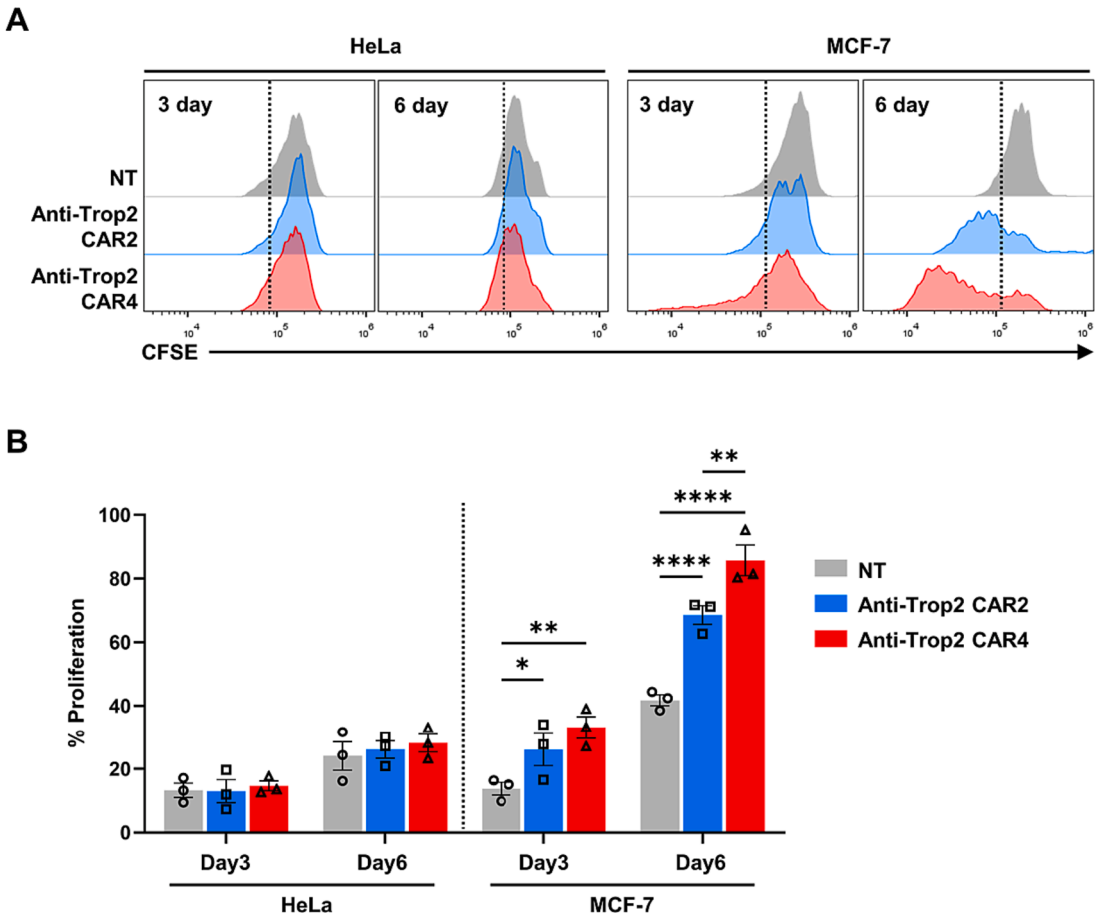

Fig. 5. Proliferative capacity of anti-Trop2 CAR2-T cells and anti-Trop2 CAR4-T cells. (A) Representative histogram illustrating CFSE dilution staining on NT-T, anti-Trop2 CAR2-T, and anti-Trop2 CAR4-T cells following exposure to HeLa cells or MCF-7 cells. (B) Bar graph summarizing the percentage of T cell proliferation, compiled from three independent experiments. Error bars indicate SEM, with results compared using two-way ANOVA. *$p < 0.05$, **$p < 0.01$, ****$p < 0.0001$.

in solid tumors are the absence of an ideal surface antigen and inadequate maintenance of CAR-T cell viability.

Trop2, a protein exhibiting elevated expression in BCs, has been associated with adverse clinical outcomes [27,28]. It is highly expressed in various cancers, including BC, with the highest levels found in TNBCs. Our research group has demonstrated substantial Trop2 expression (89.5 %) in pathological tissue samples from BC patients (submitted manuscript), suggesting its potential as a promising cancer antigen for BC.

Furthermore, Trop2-targeted antibody-drug conjugates (ADCs) have shown promising results in clinical trials across different tumor types, including refractory cases like TNBCs [35]. Therefore, Trop2 emerges as a compelling candidate antigen for CAR-T cell therapy in BC. In this regard, we assessed Trop2 surface expression in BC cell lines to evaluate its suitability for CAR-T cell therapy. Our investigations revealed the presence of Trop2 in both triple negative (MDA-MB-231 and HCC70) and luminal (MCF-7) BC subtypes, while its expression was absent in the cervical cancer HeLa cell line (Fig. 1). Consequently, HeLa cells were chosen as negative target cells, while MDA-MB-231, HCC70, and MCF-7 cells were selected as positive target cells, exhibiting varying levels of Trop2 expression. This selection allows for a comprehensive assessment of CAR-T cell efficacy.

Prior investigations have documented the utilization of CD27-based anti-Trop2 CAR-T cells in BC and similar solid tumor contexts [30]. Although these CAR-T cells have demonstrated tumor growth inhibition *in vivo*, they have not achieved complete remission in murine models with tumors. In our earlier studies, we innovated fourth-generation CAR-T cells that incorporate three distinct costimulatory domains (CD28/4-1BB/CD27) and assessed their performance in both cholangiocarcinoma [16–18] and BC [15]. The results highlighted that fourth-generation CAR-T cells exhibited superior efficacy in inhibiting tumor progression compared to counterparts featuring only CD28 or 4-1BB signaling domains. Comparative analyses have confirmed the superior benefits of fourth-generation CARs over second- and third-generations counterparts [31]. Given these observations, the use of a fourth-generation CAR targeting Trop2 presents itself as a feasible and potent strategy for BC treatment. The effectiveness of CAR-T cells relies on their ability to accurately identify and bind to specific target antigens on the surfaces of cancer cell [36].

In our investigation, we employed distinct co-stimulatory molecules with established roles in regulating various aspects of CAR-T cell behavior, including anti-tumor efficacy, cellular proliferation, cytokine generation, and viability. To achieve this, we engineered a lentiviral pCDH vector to incorporate the scFv derived from the Trop2- targeting antibody drug conjugate, which has been approved by FDA for treating unresectable locally advanced or metastatic TNBC [32]. This scFv was subsequently fused with a CAR module consisting of CD28, 4-1BB, CD27, and CD3ζ domains, resulting in the creation of anti-Trop2-CAR4 construct in comparison to anti-Trop2 CAR2, which includes only CD28 (Fig. 2A). CD28, present in both quiescent and activated T cells, has demonstrated the ability to foster T cell amplification, IL-2 secretion, and production of Th1 cytokines, and resilience against activation-induced cell death (AICD) in CAR-T cells [37]. CAR-T cells incorporating CD28 have evinced heightened anti-cancer functions and durability both *in vitro* and *in vivo*, surpassing their first-generation CAR-T counterparts or those solely reliant on the 4-1BB co-stimulatory

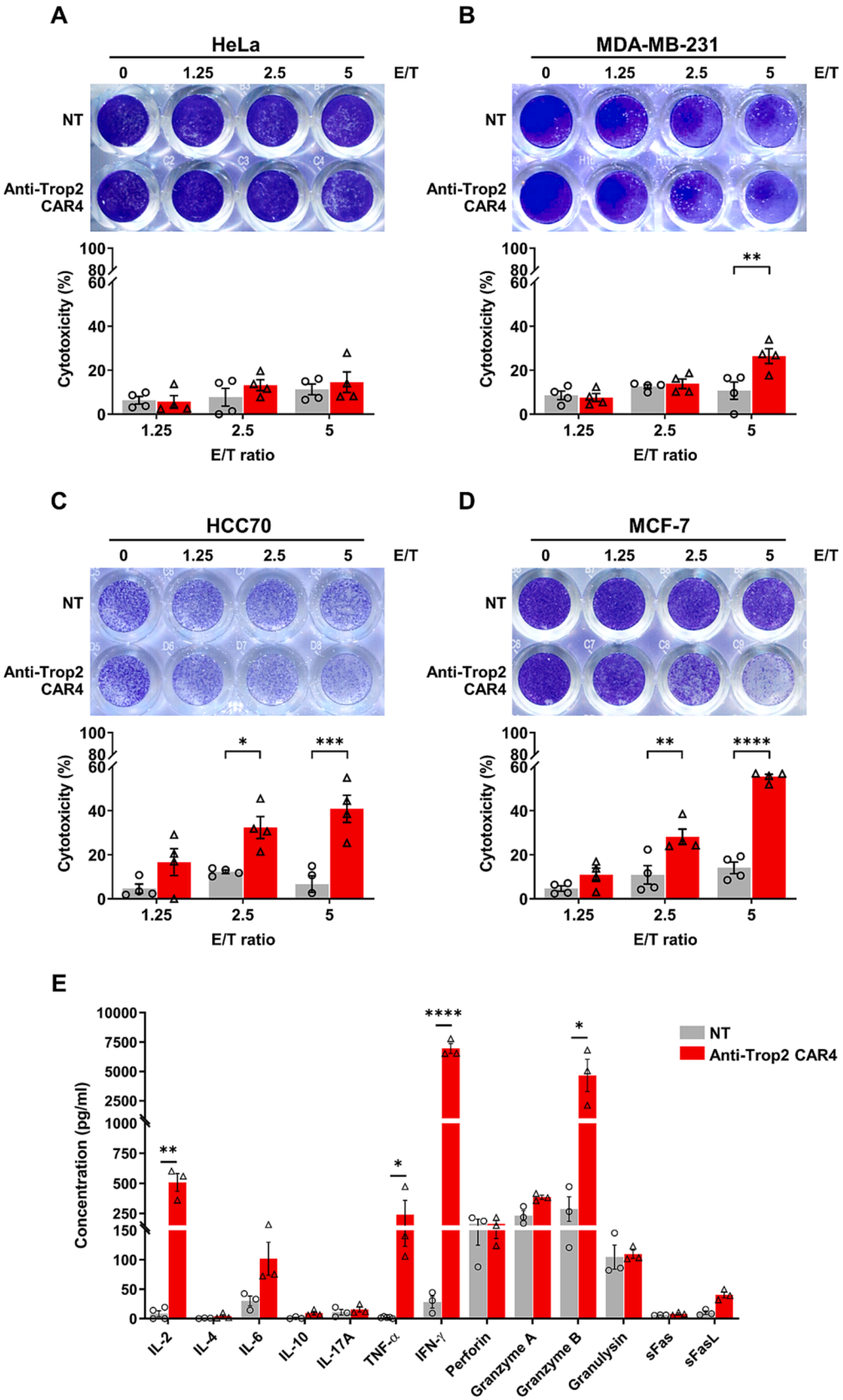

(caption on next page)

Fig. 6. Short-term cytotoxicity and cytokine secretion profiling of anti-Trop2 CAR4-T cells against Trop2-expressing BC cell lines. (A, B, C, D) Crystal violet staining was conducted on HeLa, MDA-MB-231, HCC70, and MCF-7 cells post co-culture with either NT-T cells or anti-Trop2 CAR4-T. The cells were co-cultured at specified E:T ratios (0, 1.25, 2.5, and 5) for a 24-h duration. The ensuing cytotoxicity percentages for each cell line are presented below the respective panels. Statistical differences were evaluated through two-way ANOVA. (E) Cytokine production levels in the supernatant of anti-Trop2 CAR4-T cells were assessed using cytometric bead array (CBA) after 24-h period of activation through culturing with BC cells at an E:T ratio of 5:1. The statistical differences were analyzed by Student *t*-test. The results from NT-T cells and anti-Trop2 CAR4-T cells are distinguished by gray and red, respectively. All dataset, derived from at least three independent experiments, is presented as mean ± SEM. $^{*}P < 0.05$, $^{**}P < 0.01$, $^{***}P < 0.001$, $^{****}P < 0.0001$.

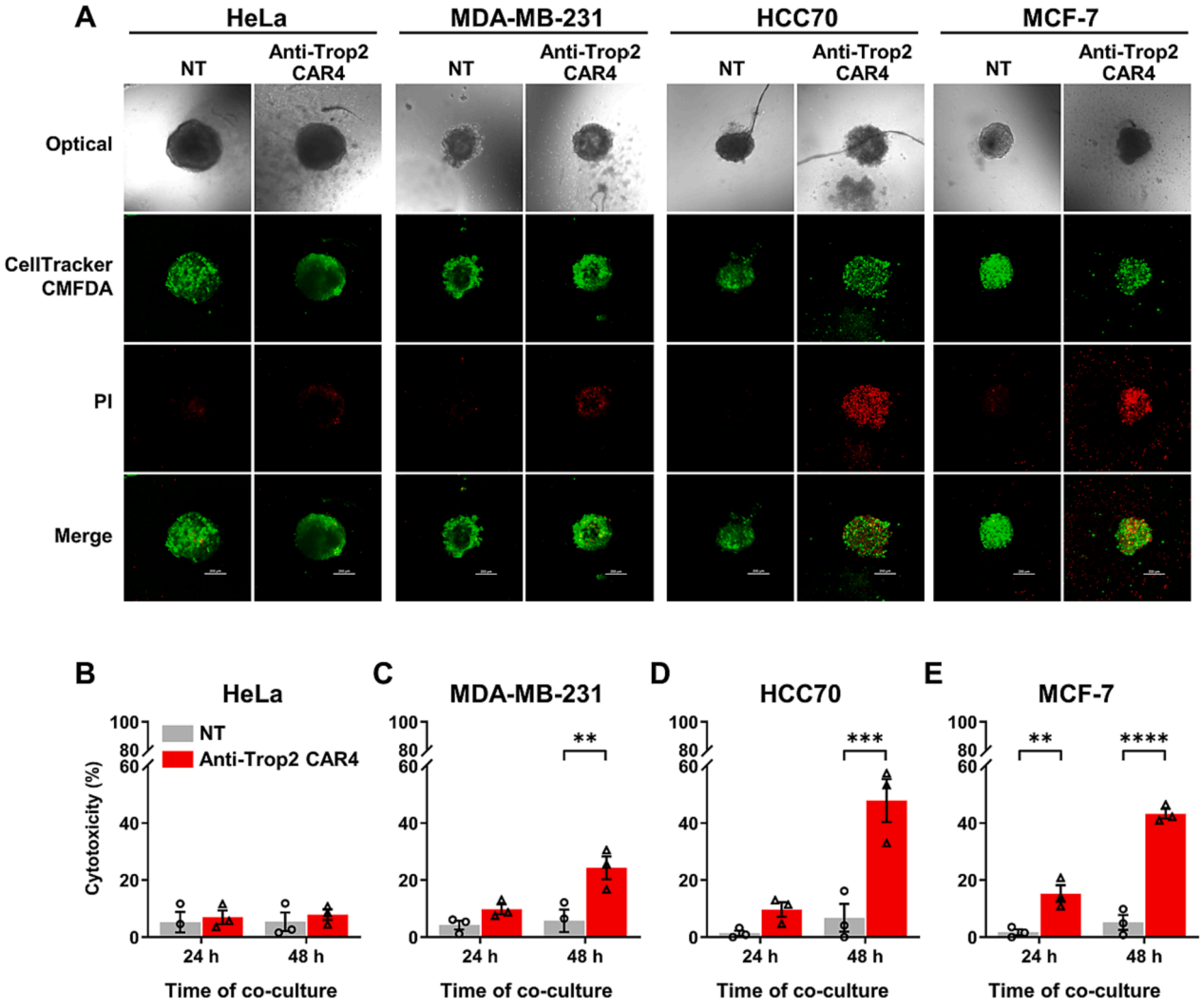

Fig. 7. Cytotoxic efficacy of anti-Trop2 CAR4-T cells against Trop2-expressing BC cell lines in a 3D spheroid model. (A) Representative fluorescence micrographs depicting the cytotoxic efficacy of NT-T cells and anti-Trop2 CAR4-T cells against CMFDA-labeled HeLa, MDA-MB-231, HCC70, and MCF-7 cells within a 3D spheroid. Deceased cells, indicated by their uptake of PI and resultant red fluorescence, are observed alongside the green CMFDA-labeled cells after co-cultured for 48 h at E:T ratio 5:1. (B, C, D, E) Assessment of cytotoxic performance conducted over 24 h and 48 h using PI incorporation to quantify cell death within spheroids, comparing NT-T cells with anti-Trop2 CAR4-T cells against HeLa, MDA-MB-231, HCC70, and MCF-7 cell lines. Standard error of the mean (SEM) is represented by error bars in all graphs, and each experimental iteration was independently replicated thrice. Significance levels are denoted as follows: $^{**}P < 0.01$, $^{***}P < 0.001$, $^{****}P < 0.0001$.

domain [38]. Furthermore, CD28 augmentation has exhibited the potential to enhance CAR-T cell performance, expansion, and persistence in lymphoma patients [39]. The 4-1BB (CD137) molecule, initially expressed in resting $CD8^+$ T cells, is upregulated following activation in both $CD4^+$ and $CD8^+$ T cells. Activation of 4-1BB intensifies IL-2 and IFN-γ production in $CD8^+$ T cells and triggers IL-2 and IL-4 secretion in $CD4^+$ T cells. It particularly advances the amplification of $CD8^+$ T cells [40], as well as the expression of granzyme B, IFN-γ, TNF-α, and resistance to programmed cell death *in vitro* [41]. Incorporating CD27 in our CAR-T cells was projected to enhance their resilience against apoptotic processes. Previous inquiries have indicated that CAR-T cells grounded on CD27 manifest heightened longevity compared to those grounded on CD28 [42]. Thus, the incorporation of these three co-stimulatory molecules (CD28, 4-1BB, and CD27) into our CAR-T cells is predicted to invigorate their anti-tumor attributes, proliferation, and persistence. We verified the presence of anti-Trop2 CAR2 and anti-Trop2 CAR4 construct in Lenti-X^{TM} HEK293T cells (Supplementary Fig. S1C) and in lentivirus-transduced T cells (Fig. 2B and C) with a notably high transduction efficiency.

The examination of cell phenotypes revealed significant shifts in the composition of immune cell populations. Notably, a decrease in NK cells and NKT cells was observed, accompanied by an increase in cytotoxic T

cells ($CD3^+/CD8^+$) (Fig. 2D). These changes in cell populations could be attributed to the presence of distinct cytokines, specifically IL-2, IL-7, and IL-15, in the cultivation milieu. Earlier research has shown that the inclusion of IL-2 or IL-15 cytokines, along with antigenic stimulation, can significantly enhance the expansion of $CD8^+$ T cells specific to the antigen [43]. Moreover, the predominant cell subset within both anti-Trop2 CAR2-T and anti-Trop2 CAR4-T cells was identified as the Tcm subtype (Fig. 2E). This increase in the Tcm subtype could be associated with the presence of IL-7 and IL-15 cytokines in the culture system. Another *in vivo* investigation has demonstrated that the sustained presence of IL-7 and IL-15 can induce the proliferation of T-memory stem cell markers in CD19 CAR-T cells [44]. These findings imply that our production procedure effectively bolstered the efficacy of anti-Trop2 CAR4-T cells by fostering the perpetuation of cytotoxic T cells ($CD3^+/CD8^+$) and Tcm phenotypes. This conservation of distinct immune cell populations is apt to contribute to the tenacity and cytotoxic prowess of CAR-T cells [45,46].

To evaluate efficacy, we compared the anti-tumor capabilities of anti-Trop2 CAR2-T and anti-Trop2 CAR4-T cells against Trop2-expressing BC cells. Our findings demonstrated that anti-Trop2 CAR4-T cells exhibited significantly heightened killing activity and an increased number of IFN-γ positive spots, a cytokine known for enhancing the motility and cytotoxicity of $CD8^+$ cytotoxic lymphocytes [47], when challenged with Trop2-expressing cells, in comparison to anti-Trop2 CAR2-T cells (Fig. 3A-C). Anti-Trop2 CAR4-T cells displayed superior early cytotoxicity against target MCF-7 cells, with markedly higher activity observed at days 2 and 4 (Fig. 4A). However, this initial advantage may diminish by day 6 due to the near depletion of target cells (supplementary Fig. S4C). Notably, CAR4-T cells consistently maintained lower PD-1 expression (Fig. 4B), indicating reduced exhaustion and potentially contributing to their sustained activity. This observation aligns with studies demonstrating 4-1BB's ability to decrease exhaustion markers in CAR-T cells [48].

Furthermore, anti-Trop2 CAR4-T cells exhibited consistently higher proliferation after long-term co-culture (Fig. 5), likely benefiting from the synergistic effects of 4-1BB and CD27 costimulatory domains, which enhance both T cell survival and expansion [49]. This suggests an enhanced capacity for long-term expansion and potentially a more robust response driven by antigen recognition. The improved proliferative capacity, possibly linked to reduced PD-1 expression, underscores the potential of CAR4-T cells for sustained anti-tumor activity. Therefore, the superior long-term cytotoxicity and proliferation of CAR4-T cells likely result from the combined benefits of the 4-1BB and CD27 costimulatory signals, making them promising candidates for further investigation against various breast cancer cells.

To ascertain the precision of anti-Trop2 CAR-T cells, we compared their cytotoxicity against HeLa cells with that of NT-T cells. The findings indicated a lack of statistically significant cytotoxic activity by anti-Trop2 CAR4-T cells against HeLa cells, affirming their specificity (Fig. 6A). Furthermore, we evaluated the anti-tumor potential of anti-Trop2 CAR4-T cells against BC, noting their highest effectiveness against MCF-7 cells (Fig. 6D), followed by HCC70 cells (Fig. 6C) and MDA-MB-231 cells (Fig. 6B), aligning with Trop2 expression levels (Fig. 1). Upon encountering tumor antigens, CAR-T cells secrete pro-inflammatory cytokines, including IL-2, TNF-α, and IFN-γ, pivotal in governing cellular growth, activation, and differentiation processes [50]. Remarkably, anti-Trop2 CAR4-T cells demonstrated significantly elevated cytokine secretion levels, encompassing IL-2, TNF-α, and IFN-γ when compared to NT-T cells (Fig. 6E), underscoring their specific response to the target antigen. CAR-T cells also engage granule-mediated apoptosis to eliminate tumor cells, where the release of cytotoxic granules, such as perforin and granzymes, by effector T cells plays a crucial role in inducing target cell apoptosis [51]. Within this study, the secretion of granzyme B from anti-Trop2 CAR4-T cells exhibited noteworthy elevation compared to NT-T cells (Fig. 6E). This observation aligns with prior research highlighting that augmented IL-2, TNF-α, and IFN-γ production culminates in robust CAR-T cell cytotoxicity [52,53]. In this study, we also adopted a 3D spheroid culture to assess the cytotoxicity of anti-Trop2 CAR4-T cells. The utilization of a Matrigel-based 3D cell culture system, which more closely emulates the *in vivo* extracellular matrix, affords a more faithful representation of the tumor microenvironment compared to conventional 2D monolayers [54]. This 3D culture approach is suitable for the preclinical evaluation of cancers in an *in vivo*-like setting. Our outcomes vividly demonstrated the successful infiltration of 3D cancer spheroids by anti-Trop2 CAR4-T cells, substantiating their potent Trop2-dependent cytotoxicity (Fig. 7). A limitation of our study is the lack of animal experiments to investigate the effects of anti-Trop2 CAR4-T cells in cancer treatment. Subsequent studies will employ animal models to assess potential adverse events, including inflammatory reactions and cytotoxicity in tumor tissues resulting from anti-Trop2 CAR4-T cells treatment. Furthermore, these models will be utilized to evaluate the impact of this treatment strategy on liver and kidney function, addressing significant challenges in the application of CAR-T therapy in solid tumors.

In summary, we have successfully engineered fourth-generation CAR-T cells that target Trop2, incorporating three costimulatory domains (CD28, 4-1BB, and CD27) to augment long-term anti-tumor activity. These anti-Trop2 CAR4-T cells have demonstrated substantial anti-tumor efficacy against Trop2-expressing BC cells in both 2D and 3D (spheroid) cultures. Our findings indicate an elevated production of the pro-apoptotic molecule granzyme B and proinflammatory cytokines IL-2, TNF-α, and IFN-γ, underscoring the potential of anti-Trop2 CAR4-T cells to effectively eliminate BC cells. This study provides the initial evidence of the potential effectiveness of anti-Trop2 CAR4-T cells in BC. The outcomes presented here contribute to the progression of CAR-T cell therapy for BC treatment, paving the way for further advancements in this domain.

Ethical approval

All protocols executed in research endeavors involving human subjects adhered meticulously to the ethical guidelines established by the institutional and/or national research oversight body, and were consistent with the principles set forth in the 1964 Helsinki Declaration, as well as subsequent revisions or equivalent ethical benchmarks. Ethical authorization for this investigation was duly conferred by the Siriraj Institutional Review Board (SIRB) situated within the Faculty of Medicine Siriraj Hospital, Mahidol University, situated in Bangkok, Thailand (COA no. Si 253/2022).

Funding

This research and innovation activity received financial support from various sources, including the Thailand Research Fund (TRF) (Grant no. IRN58W0001), and the Center of Excellence on Medical Biotechnology (CEMB), under the aegis of the S&T Postgraduate Education and Research Development Office, Office of Higher Education Commission (OHEC) in Thailand (Grant no. CB-61–006-01). CS received support from Mahidol University (Grant no. R016520008), while MJ was the recipient of Siriraj Chalermphrakiat Grants.

CRediT authorship contribution statement

Chalermchai Somboonpatarakun: Conceptualization, Data curation, Formal analysis, Methodology, Writing – original draft. **Nattaporn Phanthaphol:** Investigation, Methodology, Validation, Writing – review & editing. **Kwanpirom Suwanchiwasiri:** Formal analysis, Investigation. **Boonyanuch Ramwarungkura:** Formal analysis, Methodology. **Pornpimon Yuti:** Formal analysis, Investigation. **Naravat Poungvarin:** Resources. **Peti Thuwajit:** Resources. **Mutita Junking:** Conceptualization, Funding acquisition, Project administration, Writing – review & editing. **Pa-thai Yenchitsomanus:** Conceptualization, Supervision,

Writing – review & editing.

Declaration of competing interest

The authors declare that they have no known competing financial interests or personal relationships that could have appeared to influence the work reported in this paper.

Data availability

Data will be made available on request.

Acknowledgments

CS, MJ, and PY are members of the Thailand Hub of Talents in Cancer Immunotherapy (TTCI). The academic endeavors of TTCI receive support from the National Research Council of Thailand (NRCT) under grant [number N35E660102]. The authors extend their gratitude to all laboratory members for their provision of experimental materials, technical support, valuable discussions, and insightful comments. Additionally, we express our sincere appreciation to the healthy volunteer blood donors who actively participated in this study.

Appendix A. Supplementary data

Supplementary data to this article can be found online at https://doi.org/10.1016/j.intimp.2024.111631.

References

[1] H. Sung, J. Ferlay, R.L. Siegel, M. Laversanne, I. Soerjomataram, A. Jemal, F. Bray, Global cancer statistics 2020: GLOBOCAN Estimates of Incidence and Mortality Worldwide for 36 Cancers in 185 Countries, CA Cancer J Clin 71 (3) (2021) 209–249.
[2] A.G. Waks, E.P. Winer, Breast cancer treatment: A Review, JAMA 321 (3) (2019) 288–300.
[3] N. Harbeck, F. Penault-Llorca, J. Cortes, M. Gnant, N. Houssami, P. Poortmans, K. Ruddy, J. Tsang, F. Cardoso, Breast cancer, Nat Rev Dis Primers 5 (1) (2019) 66.
[4] G. Gu, D. Dustin, S.A. Fuqua, Targeted therapy for breast cancer and molecular mechanisms of resistance to treatment, Curr Opin Pharmacol 31 (2016) 97–103.
[5] M. Schuster, A. Nechansky, R. Kircheis, Cancer immunotherapy, Biotechnol J 1 (2) (2006) 138–147.
[6] S. Feins, W. Kong, E.F. Williams, M.C. Milone, J.A. Fraietta, An introduction to chimeric antigen receptor (CAR) T-cell immunotherapy for human cancer, Am J Hematol 94 (S1) (2019) S3–S9.
[7] S.L. Maude, T.W. Laetsch, J. Buechner, S. Rives, M. Boyer, H. Bittencourt, P. Bader, M.R. Verneris, H.E. Stefanski, G.D. Myers, M. Qayed, B. De Moerloose, H. Hiramatsu, K. Schlis, K.L. Davis, P.L. Martin, E.R. Nemecek, G.A. Yanik, C. Peters, A. Baruchel, N. Boissel, F. Mechinaud, A. Balduzzi, J. Krueger, C.H. June, B.L. Levine, P. Wood, T. Taran, M. Leung, K.T. Mueller, Y. Zhang, K. Sen, D. Lebwohl, M.A. Pulsipher, S.A. Grupp, Tisagenlecleucel in children and young adults with B-Cell lymphoblastic leukemia, N Engl J Med 378 (5) (2018) 439–448.
[8] S.S. Neelapu, F.L. Locke, N.L. Bartlett, L.J. Lekakis, D.B. Miklos, C.A. Jacobson, I. Braunschweig, O.O. Oluwole, T. Siddiqi, Y. Lin, J.M. Timmerman, P.J. Stiff, J. W. Friedberg, I.W. Flinn, A. Goy, B.T. Hill, M.R. Smith, A. Deol, U. Farooq, P. McSweeney, J. Munoz, I. Avivi, J.E. Castro, J.R. Westin, J.C. Chavez, A. Ghobadi, K.V. Komanduri, R. Levy, E.D. Jacobsen, T.E. Witzig, P. Reagan, A. Bot, J. Rossi, L. Navale, Y. Jiang, J. Aycock, M. Elias, D. Chang, J. Wiezorek, W. Y. Go, Axicabtagene ciloleucel CAR T-cell therapy in refractory large B-cell lymphoma, N Engl J Med 377 (26) (2017) 2531–2544.
[9] M. Wang, J. Munoz, A. Goy, F.L. Locke, C.A. Jacobson, B.T. Hill, J.M. Timmerman, H. Holmes, S. Jaglowski, I.W. Flinn, P.A. McSweeney, D.B. Miklos, J.M. Pagel, M. J. Kersten, N. Milpied, H. Fung, M.S. Topp, R. Houot, A. Beitinjaneh, W. Peng, L. Zheng, J.M. Rossi, R.K. Jain, A.V. Rao, P.M. Reagan, KTE-X19 CAR T-cell therapy in relapsed or refractory mantle-cell lymphoma, N Engl J Med 382 (14) (2020) 1331–1342.
[10] J.S. Abramson, M.L. Palomba, L.I. Gordon, M.A. Lunning, M. Wang, J. Arnason, A. Mehta, E. Purev, D.G. Maloney, C. Andreadis, A. Sehgal, S.R. Solomon, N. Ghosh, T.M. Albertson, J. Garcia, A. Kostic, M. Mallaney, K. Ogasawara, K. Newhall, Y. Kim, D. Li, T. Siddiqi, Lisocabtagene maraleucel for patients with relapsed or refractory large B-cell lymphomas (TRANSCEND NHL 001): a multicentre seamless design study, Lancet 396 (10254) (2020) 839–852.
[11] S.J. Schuster, CD19-directed CAR T cells gain traction, Lancet Oncol 20 (1) (2019) 2–3.
[12] P. Bajgain, S. Tawinwung, L. D'Elia, S. Sukumaran, N. Watanabe, V. Hoyos, P. Lulla, M.K. Brenner, A.M. Leen, J.F. Vera, CAR T cell therapy for breast cancer: harnessing the tumor milieu to drive T cell activation, J Immunother Cancer 6 (1) (2018) 34.
[13] S. Wilkie, G. Picco, J. Foster, D.M. Davies, S. Julien, L. Cooper, S. Arif, S.J. Mather, J. Taylor-Papadimitriou, J.M. Burchell, J. Maher, Retargeting of human T cells to tumor-associated MUC1: the evolution of a chimeric antigen receptor, J Immunol 180 (7) (2008) 4901–4909.
[14] O.O. Yeku, T.J. Purdon, M. Koneru, D. Spriggs, R.J. Brentjens, Armored CAR T cells enhance antitumor efficacy and overcome the tumor microenvironment, Sci Rep 7 (1) (2017) 10541.
[15] P. Luangwattananun, M. Junking, J. Sujjitjoon, Y. Wutti-In, N. Poungvarin, C. Thuwajit, P.T. Yenchitsomanus, Fourth-generation chimeric antigen receptor T cells targeting folate receptor alpha antigen expressed on breast cancer cells for adoptive T cell therapy, Breast Cancer Res Treat 186 (1) (2021) 25–36.
[16] N. Phanthaphol, C. Somboonpatarakun, K. Suwanchiwasiri, T. Chieochansin, J. Sujjitjoon, S. Wongkham, J. Maher, M. Junking, P.T. Yenchitsomanus, Chimeric antigen receptor T cells targeting integrin αvβ6 expressed on cholangiocarcinoma cells, Front Oncol 11 (2021) 657868.
[17] T. Sangsuwannukul, K. Supimon, J. Sujjitjoon, N. Phanthaphol, T. Chieochansin, N. Poungvarin, S. Wongkham, M. Junking, P.T. Yenchitsomanus, Anti-tumour effect of the fourth-generation chimeric antigen receptor T cells targeting CD133 against cholangiocarcinoma cells, Int Immunopharmacol 89 (Pt B) (2020) 107069.
[18] K. Supimon, T. Sangsuwannukul, J. Sujjitjoon, N. Phanthaphol, T. Chieochansin, N. Poungvarin, S. Wongkham, M. Junking, P.T. Yenchitsomanus, Anti-mucin 1 chimeric antigen receptor T cells for adoptive T cell therapy of cholangiocarcinoma, Sci Rep 11 (1) (2021) 6276.
[19] Y.H. Yang, J.W. Liu, C. Lu, J.F. Wei, CAR-T Cell Therapy for Breast Cancer: From Basic Research to Clinical Application, Int J Biol Sci 18 (6) (2022) 2609–2626.
[20] D. Fong, P. Moser, C. Krammel, J.M. Gostner, R. Margreiter, M. Mitterer, G. Gastl, G. Spizzo, High expression of TROP2 correlates with poor prognosis in pancreatic cancer, Br J Cancer 99 (8) (2008) 1290–1295.
[21] Y.J. Fang, Z.H. Lu, G.Q. Wang, Z.Z. Pan, Z.W. Zhou, J.P. Yun, M.F. Zhang, D. S. Wan, Elevated expressions of MMP7, TROP2, and survivin are associated with survival, disease recurrence, and liver metastasis of colon cancer, Int J Colorectal Dis 24 (8) (2009) 875–884.
[22] E. Bignotti, P. Todeschini, S. Calza, M. Falchetti, M. Ravanini, R.A. Tassi, A. Ravaggi, E. Bandiera, C. Romani, L. Zanotti, G. Tognon, F.E. Odicino, F. Facchetti, S. Pecorelli, A.D. Santin, Trop-2 overexpression as an independent marker for poor overall survival in ovarian carcinoma patients, Eur J Cancer 46 (5) (2010) 944–953.
[23] W. Zhao, H. Zhu, S. Zhang, H. Yong, W. Wang, Y. Zhou, B. Wang, J. Wen, Z. Qiu, G. Ding, Z. Feng, J. Zhu, Trop2 is overexpressed in gastric cancer and predicts poor prognosis, Oncotarget 7 (5) (2016) 6136–6145.
[24] A. Bardia, I.A. Mayer, J.R. Diamond, R.L. Moroose, S.J. Isakoff, A.N. Starodub, N. C. Shah, J. O'Shaughnessy, K. Kalinsky, M. Guarino, V. Abramson, D. Juric, S. M. Tolaney, J. Berlin, W.A. Messersmith, A.J. Ocean, W.A. Wegener, P. Maliakal, R. M. Sharkey, S.V. Govindan, D.M. Goldenberg, L.T. Vahdat, Efficacy and Safety of Anti-Trop-2 Antibody Drug Conjugate Sacituzumab Govitecan (IMMU-132) in Heavily Pretreated Patients With Metastatic Triple-Negative Breast Cancer, J Clin Oncol 35 (19) (2017) 2141–2148.
[25] H. Lin, H. Zhang, J. Wang, M. Lu, F. Zheng, C. Wang, X. Tang, N. Xu, R. Chen, D. Zhang, P. Zhao, J. Zhu, Y. Mao, Z. Feng, A novel human Fab antibody for Trop2 inhibits breast cancer growth in vitro and in vivo, Int J Cancer 134 (5) (2014) 1239–1249.
[26] L. Zhang, W. Zhou, V.E. Velculescu, S.E. Kern, R.H. Hruban, S.R. Hamilton, B. Vogelstein, K.W. Kinzler, Gene expression profiles in normal and cancer cells, Science 276 (5316) (1997) 1268–1272.
[27] J. Wang, R. Day, Y. Dong, S.J. Weintraub, L. Michel, Identification of Trop-2 as an oncogene and an attractive therapeutic target in colon cancers, Mol Cancer Ther 7 (2) (2008) 280–285.
[28] H. Lin, J.F. Huang, J.R. Qiu, H.L. Zhang, X.J. Tang, H. Li, C.J. Wang, Z.C. Wang, Z. Q. Feng, J. Zhu, Significantly upregulated TACSTD2 and Cyclin D1 correlate with poor prognosis of invasive ductal breast cancer, Exp Mol Pathol 94 (1) (2013) 73–78.
[29] S. Wahby, L. Fashoyin-Aje, C.L. Osgood, J. Cheng, M.H. Fiero, L. Zhang, S. Tang, S. S. Hamed, P. Song, R. Charlab, S.E. Dorff, T.K. Ricks, K. Barnett-Ringgold, J. Dinin, K.B. Goldberg, M.R. Theoret, R. Pazdur, L. Amiri-Kordestani, J.A. Beaver, FDA Approval Summary: Accelerated Approval of Sacituzumab Govitecan-hziy for Third-line Treatment of Metastatic Triple-negative Breast Cancer, Clin Cancer Res 27 (7) (2021) 1850–1854.
[30] H. Chen, F. Wei, M. Yin, Q. Zhao, Z. Liu, B. Yu, Z. Huang, CD27 enhances the killing effect of CAR T cells targeting trophoblast cell surface antigen 2 in the treatment of solid tumors, Cancer Immunol Immunother 70 (7) (2021) 2059–2071.
[31] Y. Wutti-In, J. Sujjitjoon, N. Sawasdee, A. Panya, K. Kongkla, P. Yuti, P. Yongpitakwattana, C. Thepmalee, M. Junking, T. Chieochansin, N. Poungvarin, M. Yamabhai, P.T. Yenchitsomanus, Development of a Novel Anti-CD19 CAR Containing a Fully Human scFv and Three Costimulatory Domains, Front Oncol 11 (2021) 802876.
[32] D.M. Goldenberg, T.M. Cardillo, S.V. Govindan, E.A. Rossi, R.M. Sharkey, Trop-2 is a novel target for solid cancer therapy with sacituzumab govitecan (IMMU-132), an antibody-drug conjugate (ADC), Oncotarget 6 (26) (2015) 22496–22512.
[33] S. Lei, R. Zheng, S. Zhang, S. Wang, R. Chen, K. Sun, H. Zeng, J. Zhou, W. Wei, Global patterns of breast cancer incidence and mortality: A population-based cancer registry data analysis from 2000 to 2020, Cancer Commun (lond) 41 (11) (2021) 1183–1194.

[34] M.V. Maus, S.A. Grupp, D.L. Porter, C.H. June, Antibody-modified T cells: CARs take the front seat for hematologic malignancies, Blood 123 (17) (2014) 2625–2635.
[35] D.M. Goldenberg, R.M. Sharkey, Sacituzumab govitecan, a novel, third-generation, antibody-drug conjugate (ADC) for cancer therapy, Expert Opin Biol Ther 20 (8) (2020) 871–885.
[36] D. Xu, G. Jin, D. Chai, X. Zhou, W. Gu, Y. Chong, J. Song, J. Zheng, The development of CAR design for tumor CAR-T cell therapy, Oncotarget 9 (17) (2018) 13991–14004.
[37] J.H. Esensten, Y.A. Helou, G. Chopra, A. Weiss, J.A. Bluestone, CD28 Costimulation: From Mechanism to Therapy, Immunity 44 (5) (2016) 973–988.
[38] C.M. Kowolik, M.S. Topp, S. Gonzalez, T. Pfeiffer, S. Olivares, N. Gonzalez, D. D. Smith, S.J. Forman, M.C. Jensen, L.J. Cooper, CD28 costimulation provided through a CD19-specific chimeric antigen receptor enhances in vivo persistence and antitumor efficacy of adoptively transferred T cells, Cancer Res 66 (22) (2006) 10995–11004.
[39] B. Savoldo, C.A. Ramos, E. Liu, M.P. Mims, M.J. Keating, G. Carrum, R.T. Kamble, C.M. Bollard, A.P. Gee, Z. Mei, H. Liu, B. Grilley, C.M. Rooney, H.E. Heslop, M. K. Brenner, G. Dotti, CD28 costimulation improves expansion and persistence of chimeric antigen receptor-modified T cells in lymphoma patients, J Clin Invest 121 (5) (2011) 1822–1826.
[40] H. Zhang, K.M. Snyder, M.M. Suhoski, M.V. Maus, V. Kapoor, C.H. June, C. L. Mackall, 4–1BB is superior to CD28 costimulation for generating CD8+ cytotoxic lymphocytes for adoptive immunotherapy, J Immunol 179 (7) (2007) 4910–4918.
[41] X.S. Zhong, M. Matsushita, J. Plotkin, I. Riviere, M. Sadelain, Chimeric antigen receptors combining 4–1BB and CD28 signaling domains augment PI3kinase/AKT/Bcl-XL activation and CD8+ T cell-mediated tumor eradication, Mol Ther 18 (2) (2010) 413–420.
[42] D.-G. Song, Q. Ye, M. Poussin, G.M. Harms, M. Figini, D.J. Powell Jr, CD27 costimulation augments the survival and antitumor activity of redirected human T cells in vivo, Blood 119 (3) (2012) 696–706.
[43] M. Montes, N. Rufer, V. Appay, S. Reynard, M.J. Pittet, D.E. Speiser, P. Guillaume, J.-C. Cerottini, P. Romero, S. Leyvraz, Optimum in vitro expansion of human antigen-specific CD8+ T cells for adoptive transfer therapy, Clin. Exp. Immunol. 142 (2) (2005) 292–302.
[44] Y. Xu, M. Zhang, C.A. Ramos, A. Durett, E. Liu, O. Dakhova, H. Liu, C.J. Creighton, A.P. Gee, H.E. Heslop, C.M. Rooney, B. Savoldo, G. Dotti, Closely related T-memory stem cells correlate with in vivo expansion of CAR.CD19-T cells and are preserved by IL-7 and IL-15, Blood 123 (24) (2014) 3750–3759.
[45] A.D. McLellan, S.M. Ali Hosseini Rad, Chimeric antigen receptor T cell persistence and memory cell formation, Immunol. Cell Biol. 97 (7) (2019) 664–674.
[46] T. Samji, K.M. Khanna, Understanding memory CD8+ T cells, Immunol. Lett. 185 (2017) 32–39.
[47] P. Bhat, G. Leggatt, N. Waterhouse, I.H. Frazer, Interferon-γ derived from cytotoxic lymphocytes directly enhances their motility and cytotoxicity, Cell Death Dis 8 (6) (2017) e2836.
[48] A.H. Long, W.M. Haso, J.F. Shern, K.M. Wanhainen, M. Murgai, M. Ingaramo, J. P. Smith, A.J. Walker, M.E. Kohler, V.R. Venkateshwara, R.N. Kaplan, G. H. Patterson, T.J. Fry, R.J. Orentas, C.L. Mackall, 4–1BB costimulation ameliorates T cell exhaustion induced by tonic signaling of chimeric antigen receptors, Nat Med 21 (6) (2015) 581–590.
[49] D. Li, X. Li, W.L. Zhou, Y. Huang, X. Liang, L. Jiang, X. Yang, J. Sun, Z. Li, W. D. Han, W. Wang, Genetically engineered T cells for cancer immunotherapy, Signal Transduct Target Ther 4 (2019) 35.
[50] X. Xiao, S. Huang, S. Chen, Y. Wang, Q. Sun, X. Xu, Y. Li, Mechanisms of cytokine release syndrome and neurotoxicity of CAR T-cell therapy and associated prevention and management strategies, J Exp Clin Cancer Res 40 (1) (2021) 367.
[51] M.R. Benmebarek, C.H. Karches, B.L. Cadilha, S. Lesch, S. Endres, S. Kobold, Killing Mechanisms of Chimeric Antigen Receptor (CAR) T Cells, Int J Mol Sci 20 (6) (2019).
[52] E. Drent, R.W. Groen, W.A. Noort, M. Themeli, J.J. Lammerts van Bueren, P. W. Parren, J. Kuball, Z. Sebestyen, H. Yuan, J. de Bruijn, N.W. van de Donk, A. C. Martens, H.M. Lokhorst, T. Mutis, Pre-clinical evaluation of CD38 chimeric antigen receptor engineered T cells for the treatment of multiple myeloma, Haematologica 101 (5) (2016) 616–625.
[53] Z. Zhang, D. Jiang, H. Yang, Z. He, X. Liu, W. Qin, L. Li, C. Wang, Y. Li, H. Li, H. Xu, H. Jin, Q. Qian, Modified CAR T cells targeting membrane-proximal epitope of mesothelin enhances the antitumor function against large solid tumor, Cell Death Dis 10 (7) (2019) 476.
[54] M. Ravi, V. Paramesh, S.R. Kaviya, E. Anuradha, F.D. Solomon, 3D cell culture systems: advantages and applications, J Cell Physiol 230 (1) (2015) 16–26.